

## Supporting Information

### Experimental and kinetic modeling study of the pyrolysis and oxidation of diethylamine

Cato Pappijn<sup>a</sup>, Nicolas Vin<sup>b</sup>, Florence H. Vermeire<sup>a</sup>, Ruben Van de Vijver<sup>a</sup>, Olivier Herbinet<sup>b</sup>, Frédérique Battin-Leclerc<sup>b</sup>, Marie-Françoise Reyniers<sup>a</sup>, Guy B. Marin<sup>a</sup>, Kevin M. Van Geem<sup>a,\*</sup>

<sup>a</sup>Laboratory for Chemical Technology, Ghent University, Technologiepark 121, 9052 Gent, Belgium

<sup>b</sup>Laboratoire Réactions et Génie des Procédés, CNRS, Université de Lorraine, Nancy, France

\*Corresponding author: Technologiepark 121, 9052 Gent, Belgium, T: +32 92645597, e-mail: [kevin.vangeem@ugent.be](mailto:kevin.vangeem@ugent.be)

# Table of contents

1. Experimental results .....	3
2. Tubular reactor .....	3
2.1 Discussion on plug flow reactor assumption .....	3
2.2 Temperatures profiles .....	3
3. Kinetic model .....	4
4. Nomenclature .....	5
5. Results of quantum chemical calculations .....	6
5.1 Thermodynamic properties calculated at the CBS-QB3 level of theory .....	6
5.2 Kinetic parameters calculated at the CBS-QB3 level of theory .....	8
6. Comparison between ab initio calculated rate coefficients and rate coefficients from the Glarborg et al. mechanism .....	9
7. Sensitivity analyses .....	11
7.1 Pyrolysis .....	11
7.2 Oxidation .....	12
8. References .....	14

## 1. Experimental results

The experimental data acquired for the pyrolysis and oxidation of diethylamine in the tubular and jet-stirred reactor, located in Nancy, France, is provided as a separate Excel spreadsheet.

## 2. Tubular reactor

### 2.1 Discussion on plug flow reactor assumption

The tubular reactor (TR) has been modelled as an ideal plug flow reactor. To justify this assumption, the dimensionless Péclet number (Pe) is calculated using Eq. S1.

$$Pe = \frac{L^2}{D\tau + \frac{QL}{48\pi D}} \quad \text{Eq. S1}$$

In Eq. S1,  $L$  is the length of the reactor,  $\tau$  is the residence time,  $D$  is the binary diffusion coefficient and  $Q$  is the volumetric flow. The calculated values for the Péclet numbers in the TR over the studied temperature range 700 K– 1000 K are given in Table S 1. Based on these numbers ranging from 219 to 114, the use of an ideal plug flow reactor can be justified.

Table S 1: Values of the Péclet number during the pyrolysis of diethylamine (0.01 diethylamine inlet mole fraction,  $\tau = 2$  s,  $P = 1.07$  bar) in the TR.

Temperature (K)	Péclet number (-)
<b>700</b>	219
<b>725</b>	207
<b>750</b>	195
<b>775</b>	184
<b>800</b>	174
<b>825</b>	164
<b>850</b>	155
<b>875</b>	147
<b>900</b>	140
<b>925</b>	133
<b>950</b>	126
<b>975</b>	120
<b>1000</b>	114

### 2.2 Temperatures profiles

For the simulations of the TR experiments, the temperature profiles measured at unreactive conditions are used as input in the PFR model. In Figure S 1, these temperature profiles are depicted for each value of the set point temperature over the range of 700 to 1000 K in increments of 25 K.

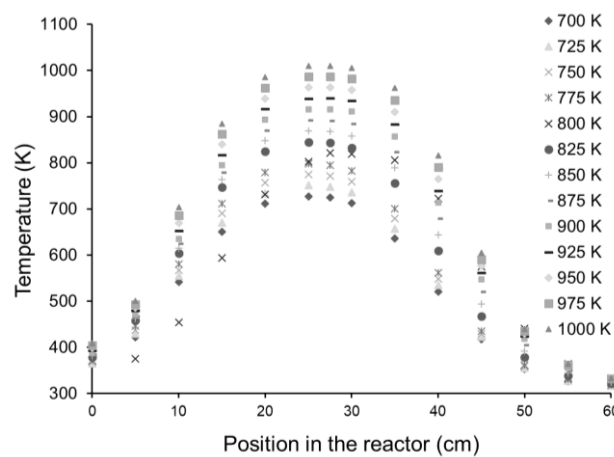


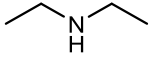
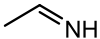
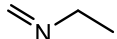
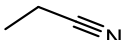
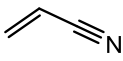
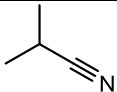
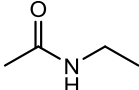
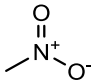
Figure S 1: Temperature profiles in the TR measured at unreactive conditions. The temperatures in the legend correspond to the set point temperatures.

### 3. Kinetic model

The kinetic model in CHEMKIN format developed for the pyrolysis and oxidation of diethylamine is provided as a separate text file.

## 4. Nomenclature

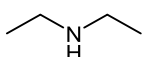
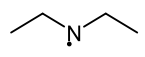
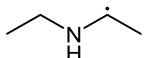
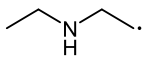
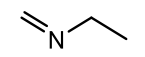
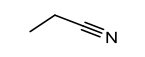
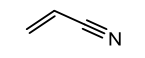
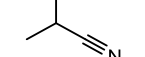
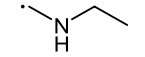
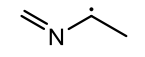
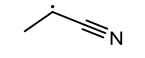
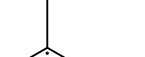
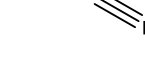
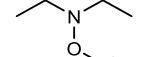
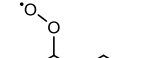
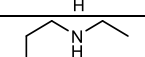
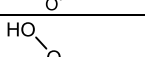
Table S 2: Nomenclature

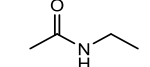
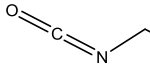
Name	Identifier	Structure
diethylamine	InChI=1S/C4H11N/c1-3-5-4-2/h5H,3-4H2,1-2H3	
methanimine	InChI=1S/CH3N/c1-2/h2H,1H2	$\text{=NH}$
ethanimine	InChI=1S/C2H5N/c1-2-3/h2-3H,1H3	
ethylmethanimine	InChI=1S/C3H7N/c1-3-4-2/h2-3H2,1H3	
propanenitrile	InChI=1S/C3H5N/c1-2-3-4/h2H2,1H3	
acetonitrile	InChI=1S/C2H3N/c1-2-3/h1H3	$\text{—}\equiv\text{N}$
acrylonitrile	InChI=1S/C3H3N/c1-2-3-4/h2H,1H2	
isobutyronitrile	InChI=1S/C4H7N/c1-4(2)3-5/h4H,1-2H3	
ethylacetamide	InChI=1S/C4H9NO/c1-3-5-4(2)6/h3H2,1-2H3,(H,5,6)	
nitromethane	InChI=1S/CH3NO2/c1-2(3)4/h1H3	

## 5. Results of quantum chemical calculations

### 5.1 Thermodynamic properties calculated at the CBS-QB3 level of theory

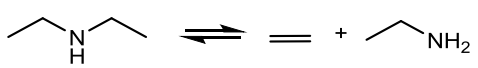
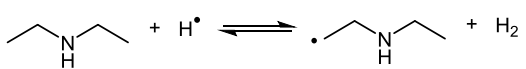
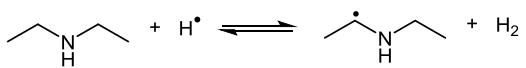
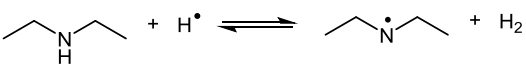
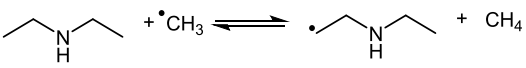
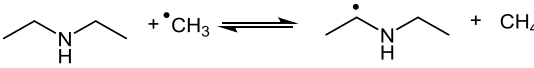
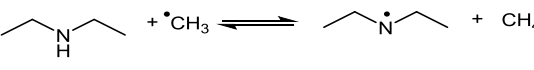
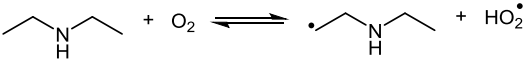
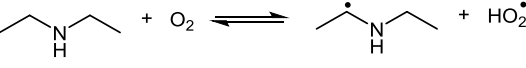
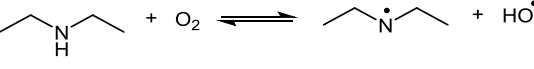
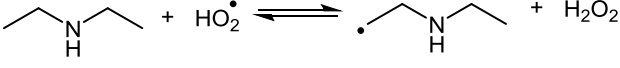
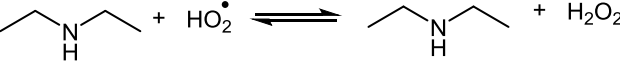
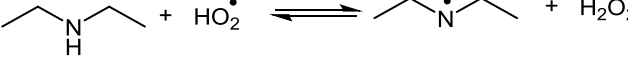
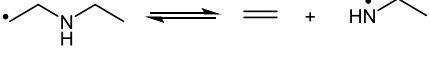
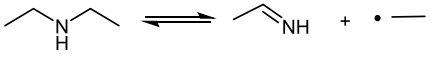
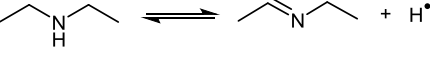
Table S 3: Thermodynamic properties for important species during the pyrolysis and oxidation of diethylamine determined with quantum chemical calculations at the CBS-QB3 level of theory.

Species	$\Delta H_f^\circ$ (298 K) [kJ mol <sup>-1</sup> ]	$S^\circ$ (298 K) [J mol <sup>-1</sup> K <sup>-1</sup> ]	Cp (500 K) [J mol <sup>-1</sup> K <sup>-1</sup> ]	Cp (600 K) [J mol <sup>-1</sup> K <sup>-1</sup> ]	Cp(800 K) [J mol <sup>-1</sup> K <sup>-1</sup> ]	Cp(1000 K) [J mol <sup>-1</sup> K <sup>-1</sup> ]
	-71.80	346.13	175.46	197.59	233.54	260.95
	103.96	355.2	164.39	185.33	219.04	244.58
	94.31	377.71	169.93	189.54	221.58	246.14
	144.50	359.2	171.68	191.21	222.87	247.07
	51.01	308.99	121.73	136.96	161.34	179.76
	57.09	285.24	102.53	114.54	133.84	148.46
	189.67	272.79	86.74	95.69	109.6	119.86
	28.44	315.28	138.7	155.05	180.95	200.44
	129.75	318.59	134.85	150.43	175.54	194.80
	188.65	300.12	113.75	127.93	150.3	166.93
	224.62	294.2	94.04	104.40	120.89	133.22
	183.70	326.58	124.54	139.72	164.16	182.46
	71.46	413.34	207.04	229.10	264.29	290.88
	-52.59	409.26	205.09	229.53	268.21	295.99
	-8.10	425.84	210.03	231.73	265.6	290.88
	-4.04	411.1	220.23	245.62	280.69	303.36
	-26.00	425.38	224.57	245.07	274.94	296.49

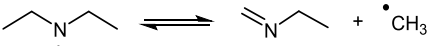
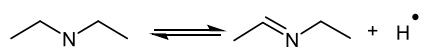
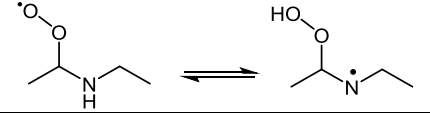
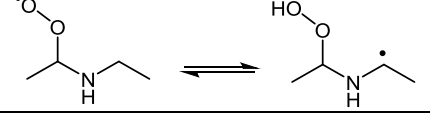
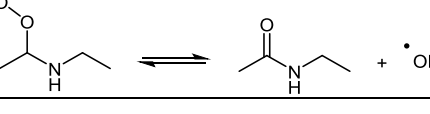
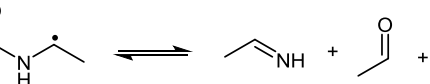
	-265.65	385.74	190.00	224.56	250.08	289.65
	-403.88	442.37	229.09	252.48	283.07	301.81

## 5.2 Kinetic parameters calculated at the CBS-QB3 level of theory

Table S 4: Kinetic parameters  $k=A\cdot T^n\cdot\exp(-B/R/T)$  for important reactions during the pyrolysis and oxidation of diethylamine determined with quantum chemical methods at the CBS-QB3 level of theory.

Reaction	A [s <sup>-1</sup> or cm <sup>3</sup> mol <sup>-1</sup> s <sup>-1</sup> ]	n	B [kJ mol <sup>-1</sup> ]
	3.70 10 <sup>11</sup>	0	281.9
	1.31 10 <sup>2</sup>	3.54	24.9
	2.04 10 <sup>1</sup>	3.71	4.7
	1.74 10 <sup>7</sup>	1.79	21.9
	5.63 10 <sup>-9</sup>	6.57	17.9
	3.52 10 <sup>-3</sup>	4.68	15.8
	8.11 10 <sup>-2</sup>	4.05	15.7
	7.76 10 <sup>1</sup>	3.68	191.9
	1.22 10 <sup>3</sup>	2.99	126.3
	2.84 10 <sup>5</sup>	2.14	140.4
	1.92 10 <sup>-4</sup>	4.55	46.7
	2.51 10 <sup>1</sup>	3.32	18.4
	3.80 10 <sup>2</sup>	3.02	21.7
	8.79 10 <sup>10</sup>	0.67	95.2
	7.31 10 <sup>13</sup>	-0.01	117.0
	1.13 10 <sup>10</sup>	0.97	144.0



	$2.20 \cdot 10^{10}$	1.01	118.5
	$3.30 \cdot 10^9$	1.33	141.2
	$1.40 \cdot 10^{-2}$	4.23	96.4
	$2.50 \cdot 10^{-3}$	4.19	46.4
	$1.14 \cdot 10^{-2}$	4.25	120.7
	$7.01 \cdot 10^{-2}$	3.67	28.0

## 6. Comparison between ab initio calculated rate coefficients and rate coefficients from the Glarborg et al. mechanism

The automatically generated model for DEA with Genesys is merged with the mechanism of Glarborg et al.[1] In the case that the same species or reactions appear in both the automatically generated Genesys mechanism and the Glarborg et al. mechanism, it is opted to retain the kinetic parameters from the Genesys mechanism. A few examples of the difference in rate coefficients when using the kinetic parameters as reported by Glarborg et al. or calculated in this work is given here. Figure S 2 depicts the Arrhenius plots for the hydrogen abstraction from ethanimine ( $\text{CH}_3\text{CHNH}$ ). It should be noted that the rate coefficients can differ several orders of magnitude depending on the temperature studied. At 600 K, i.e. the temperature at which the conversion of DEA starts at oxidation conditions, the ab initio calculated rate coefficient for hydrogen abstraction from the N-H bond is a factor of 100 larger compared to the one reported by Glarborg et al. At 1000 K, this deviation is decreased to a factor of 20. Besides the large differences in rate coefficients, the relative importance of each of the hydrogen abstraction sites differs between models, which can have a large influence on the kinetic model predictions.

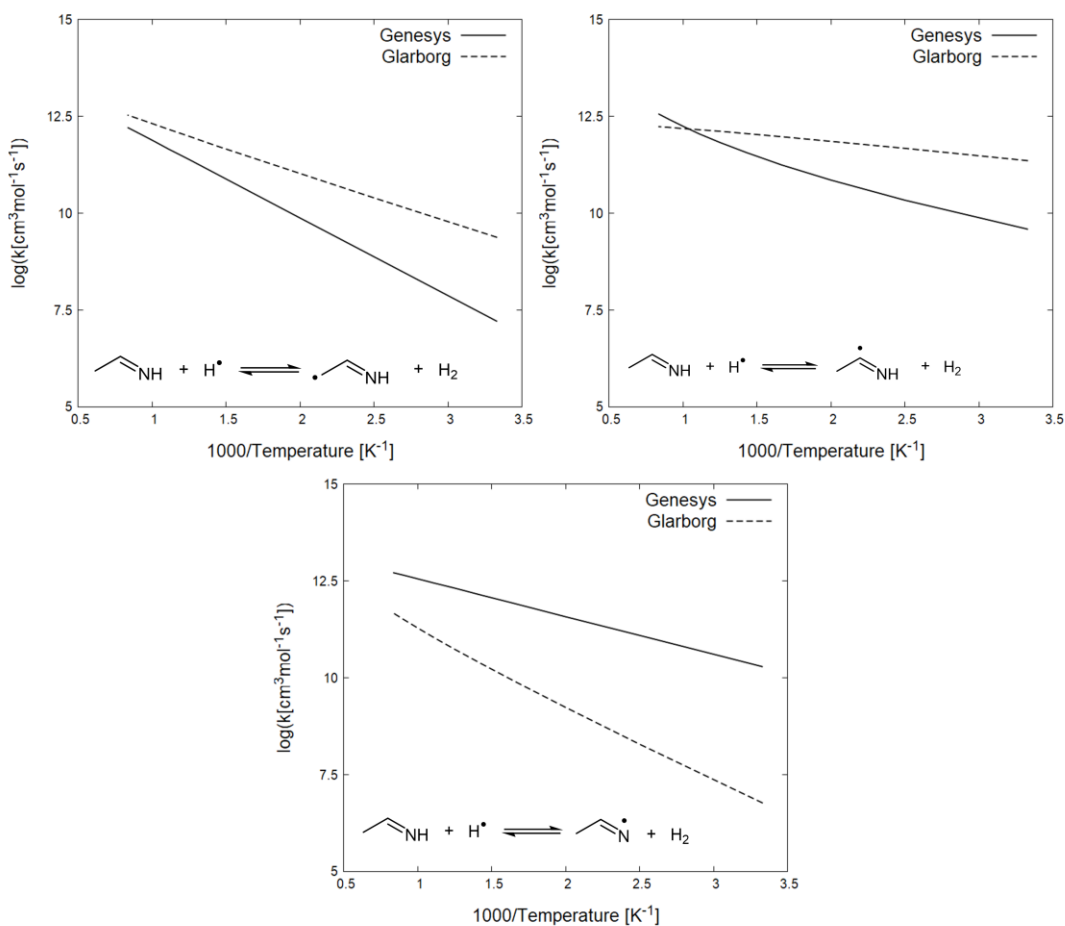


Figure S 2: Arrhenius plot for the hydrogen abstraction from ethanimine ( $\text{CH}_3\text{CHNH}$ ) by a hydrogen atom, comparing the rate coefficients obtained from ab initio calculations (Genesys) and reported in the Glarborg et al. model (Glarborg).

Figure S 3 depicts an Arrhenius plot of the C-H and C-C  $\beta$ -scissions of the radical  $\text{CH}_3\text{CHNH}^\bullet$  using the newly calculated ab initio kinetic parameters and the kinetic parameters used in the Glarborg et al. model. The kinetic parameters for the C-H  $\beta$ -scission are based on the analogous reaction of  $\text{CH}_2\text{NH}^\bullet$ , while for the C-C  $\beta$ -scission they are based on  $\text{CH}_3\text{CH}_2\text{O}^\bullet$ . It should be noted that in both models, the rate coefficient of the C-C  $\beta$ -scission is larger than the C-H  $\beta$ -scission.

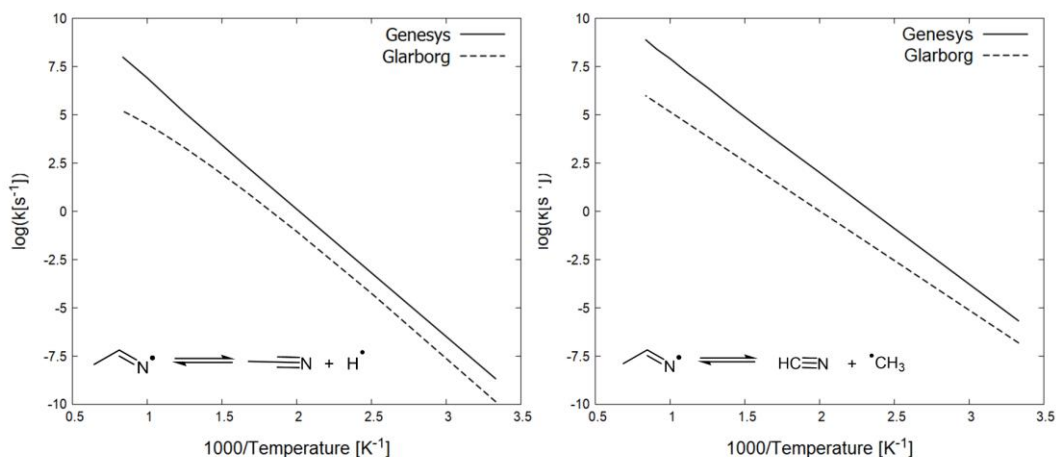


Figure S 3: Arrhenius plot for the C-H and C-C  $\beta$ -scissions of the  $\text{CH}_3\text{CH}_2\text{NH}^\bullet$  radical comparing the rate coefficients obtained from ab initio calculations (Genesys) and reported in the Glarborg et al. model (Glarborg).

Figure S 4 illustrates the influence of the accuracy of these rate coefficients on the simulated mole fractions of HCN for the oxidation of DEA at  $\varphi = 1.0$ .

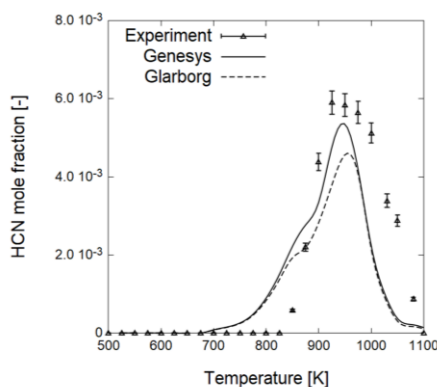


Figure S 4: Simulated mole fraction of HCN during the oxidation of DEA for  $\varphi = 1.0$  using the respective rate coefficients for the C-C  $\beta$ -scission from the Genesys and Glarborg et al. model.

## 7. Sensitivity analyses

Sensitivity analyses are performed to better understand the reaction pathways responsible for the consumption of DEA and the formation of the main product species. In the presented sensitivity analyses, a positive sensitivity coefficient for a given reaction indicates that increasing the associated pre-exponential factor increases the mole fraction of the target molecule. Analogously, a negative sensitivity coefficient for a given reaction indicates that increasing the associated pre-exponential factor decreases the mole fraction of the target molecule.

### 7.1 Pyrolysis

The sensitivity analysis with respect to the mole fraction profile of DEA for pyrolysis conditions at  $T = 800, 900$  and  $1000$  K is displayed in Figure S 5. The consumption of DEA is very sensitive towards the homolytic scission of the C-N bond. This scission increases the number of radicals in the reactive system and hence has a significant promoting effect on the

reactivity. Hydrogen atoms are formed after  $\beta$ -scission of the ethyl and ethylamine ( $\text{CH}_3\text{CH}_2\text{NH}^\bullet$ ) radicals. The homolytic scission of the C-C bond, for which the bond dissociation energy is  $5 \text{ kJ mol}^{-1}$  higher compared to C-N, results in the formation of the less reactive methyl radicals. Hydrogen abstractions by hydrogen atoms and methyl radicals from DEA have a negative sensitivity coefficient and promote the conversion of DEA. The recombination of two methyl radicals has a negative sensitivity coefficient as it results in a decrease of the number of radicals in the reactive system.

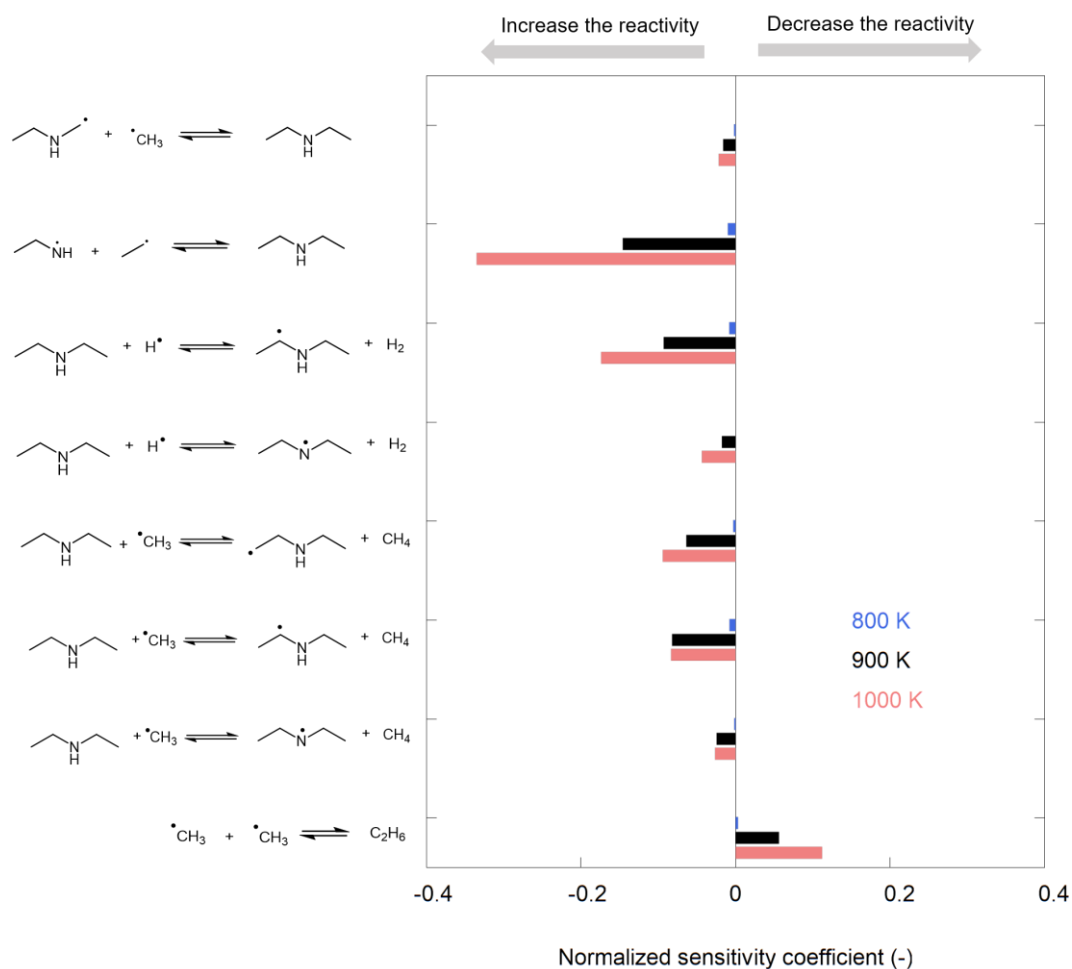


Figure S 5: Normalized sensitivity coefficients for the mole fraction of diethylamine (DEA) in DEA pyrolysis. Experimental conditions correspond to  $P = 1.07 \text{ bar}$ ,  $x_{\text{DEA},0} = 0.01$ ,  $T = 800 \text{ K}$  (blue),  $900 \text{ K}$  (black) and  $1000 \text{ K}$  (red).

## 7.2 Oxidation

The sensitivity analysis with respect to the mole fraction of DEA for oxidation at  $\phi = 1$  and  $T = 650, 750$  and  $850 \text{ K}$  is displayed in Figure S 6. The sensitive reactions include hydrogen abstraction reactions by molecular oxygen, hydroxyl radicals and hydroperoxy radicals. Most of these reactions have a negative sensitivity coefficient, as they contribute to the consumption of DEA. At  $650$  and  $750 \text{ K}$ , the main abstracting species is the hydroperoxy radical, which is in agreement with the larger sensitivity coefficient for these reactions. This radical is mainly formed via reactions of methyl and ethyl radicals, which result from the  $\beta$ -scission of fuel radicals. At approximately  $750 \text{ K}$ , the  $\beta$ -scission of the fuel radicals become more favored compared to  $\text{O}_2$  addition, leading to an increased production of these hydroperoxy radicals. Also important for the low-temperature reactivity are reactions of methyl peroxy radicals. Hydrogen abstraction by this radical forms methylhydrogenperoxide.

After homolytic scission, this species can lead to chain branching, forming the reactive hydroxyl radical and enhancing the reactivity. From Figure S 6, it can be seen that the formation of methylhydrogenperoxide corresponds to a positive sensitivity coefficient for DEA, or equivalently a reduced reactivity of DEA. Self-reaction of hydroperoxy radicals giving hydrogen peroxide and molecular oxygen has a positive sensitivity coefficient as this results in a decrease of radicals in the system. This is also the case for the recombination of a methyl and hydroperoxy radical.

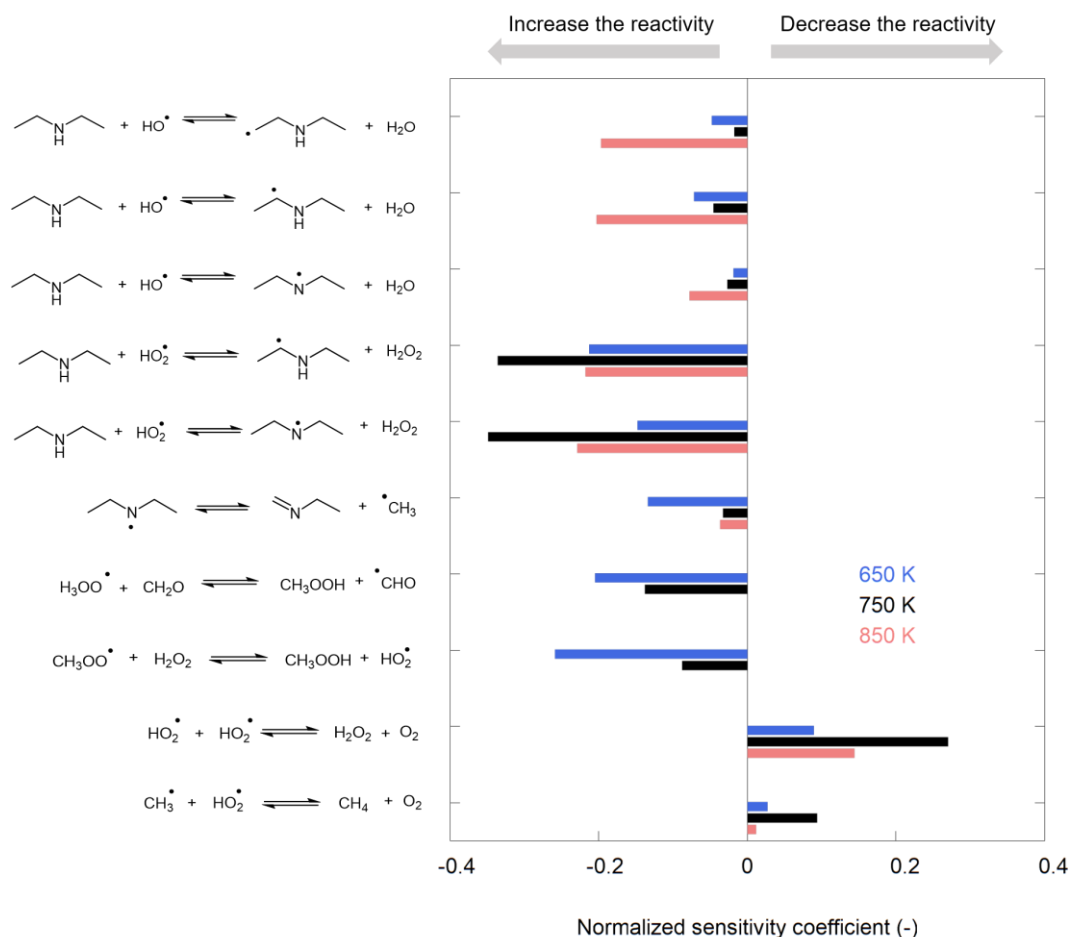


Figure S 6: Normalized sensitivity coefficients for the mole fraction of diethylamine (DEA) in DEA oxidation. Experimental conditions are  $\phi = 1$ , 1.07 bar,  $x_{\text{DEA},0} = 0.01$ ,  $T = 650$  K (blue), 750 K (black) and 850 K (red).

The sensitivity analysis with respect to the mole fractions of NO, NO<sub>2</sub> and nitromethane (CH<sub>3</sub>NO<sub>2</sub>) for oxidation at  $\phi = 1$  and  $T = 900$  K is displayed in Figure S 7. The formation of NO is very sensitive to the reaction between the imine radical (CH<sub>2</sub>N<sup>•</sup>) and molecular oxygen (R4). A higher pre-exponential coefficient for this reaction increases the formation of NO. At the same time, the competing C-H β-scission of CH<sub>2</sub>N<sup>•</sup> to HCN (R7) has a strongly negative sensitivity coefficient with respect to the NO mole fraction. The hydrogen abstraction by a hydroxyl radical and hydrogen atom from methanimine (CH<sub>2</sub>NH) increases formation of the imine radical and subsequently the formation of NO, hence the positive sensitivity coefficient for reactions R5 and R6. NO<sub>2</sub> is formed via the reaction of NO with the hydroxyl radical (R1). This direct formation explains the sensitivity coefficient for this reaction. For the other reactions listed in Figure S 7, the sensitivity coefficient of NO<sub>2</sub> is strongly correlated to the sensitivity coefficient of NO, as a production rate of NO results in a higher production rate of NO<sub>2</sub>. Nitromethane is mainly formed by the reaction between a methyl radical and NO<sub>2</sub> and

hence the competitive reaction leading the formation of methoxy radical and NO (R3) has a negative sensitivity coefficient for the mole fraction of nitromethane.

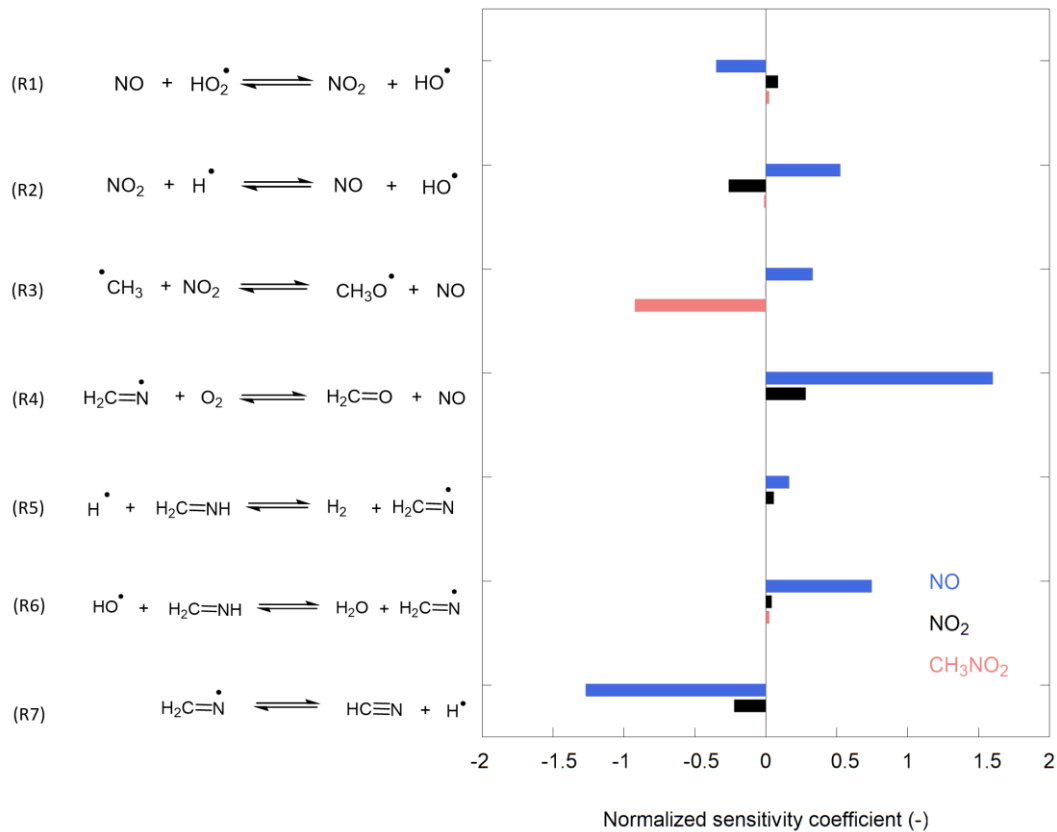


Figure S 7: Normalized sensitivity coefficients for the mole fractions NO, NO<sub>2</sub> and nitromethane (CH<sub>3</sub>NO<sub>2</sub>) in DEA oxidation. Experimental conditions are and  $\phi = 1$ , 1.07 bar,  $x_{\text{DEA},0} = 0.01$  an  $T = 900$  K.

## 8. References

[1] P. Glarborg, J.A. Miller, B. Ruscic, S.J. Klippenstein, Modeling nitrogen chemistry in combustion, *Progress in Energy and Combustion Science*, 67 (2018) 31-68.